Investigation of the Functional Contributions of Invariant Serine Residues in Yeast Mevalonate Diphosphate Decarboxylase†

Dmitriy V. Krepkiy and Henry M. Miziorko*

Department of Biochemistry, Medical College of Wisconsin, Milwaukee, Wisconsin 53226, and Division of Molecular Biology and Biochemistry, School of Biological Sciences, University of Missouri-Kansas City, Kansas City, Missouri 64110

Received July 23, 2004; Revised Manuscript Received October 19, 2004

ABSTRACT: Alignment of more than 20 deduced sequences for mevalonate diphosphate decarboxylase (MDD) indicates that serines 34, 36, 120,121, 153, and 155 are invariant residues that map within a proposed interdomain active site cleft. To test possible active site roles for these invariant serines, each has been mutated to alanine. S34A exhibits limited solubility and impaired binding of the fluorescent ATP analogue, trinitrophenyl-ATP (TNP-ATP), suggesting that Ser-34 substitution destabilizes proper enzyme folding. All other serine mutants retain structural integrity, as indicated by their ability to bind TNP-ATP at levels comparable to wild-type enzyme. S153A exhibits a 18-fold inflation in K_d for Mg-ATP, as indicated by competitive displacement of TNP-ATP; the enzyme also is characterized by a 35-fold inflation in K_m for Mg-ATP. S155A exhibits a 26-fold inflation in K_m for Mg-ATP, but competitive displacement of TNP-ATP indicates only a 2-fold inflation in K_d for this substrate. S155A exhibits both a 16-fold inflation in K_m for mevalonate diphosphate and a 14-fold inflation in $K_{i(slope)}$ for the substrate analogue, diphosphoglycolylproline. These observations suggest roles for Ser-153 and Ser-155 in substrate binding. Catalytic consequences of mutating invariant serines 36, 120, 153, and 155 are modest (<8-fold diminution in k_{cat}). In contrast, S121A, which exhibits only modest changes in K_d for Mg-ATP and K_m for mevalonate diphosphate, is characterized by a >42 000-fold diminution in k_{cat}, indicating the critical involvement of Ser-121 in reaction catalysis. The selective involvement of the latter of two tandem serine residues (Ser-120, Ser-121) in a conserved sequence motif suggests mechanistic similarities within the GHMP kinase superfamily of proteins.

Mevalonate diphosphate decarboxylase (MDD,[1] EC 4.1.1.33) catalyzes the decarboxylation reaction of mevalonate diphosphate to isopentenyl diphosphate with concurrent hydrolysis of ATP to form ADP and inorganic phosphate. The reaction (eq 1) requires divalent metal ions, e.g. Mg^{2+} or Mn^{2+} (*1*, *2*).

$$\text{Mevalonate-5-diphosphate} + \text{ATP} \rightarrow \text{Isopentenyl-5-diphosphate} + \text{ADP} + P_i + CO_2 \quad (1)$$

This reaction is critical to the biosynthetic pathway for isoprenoids and sterols. Both enzyme inhibition and diminished cellular levels of mevalonate diphosphate decarboxylase have been demonstrated to diminish cholesterol production (*3*−*5*).

The mevalonate pathway for isoprenoid biosynthesis functions in both eukaryotes and prokaryotes. The availability of more than 20 deduced MDD sequences from diverse organisms has facilitated the identification of invariant amino acid residues.

The potential significance of some of these residues is illustrated by our recent analysis of the contributions of conserved Lys-18 and Asp-302 to MDD function (*6*). A high-resolution structure of unliganded MDD (*7*) has been reported, and while the lack of bound metabolites or analogues limits the functional information that would otherwise be available, the enzyme clearly folds like members of the GHMP kinase family. A deep interdomain cleft associated with the catalytic site has been identified. Six invariant MDD serine residues map within this cleft and have the potential to support substrate binding (*8*, *9*) or catalysis (*10*, *11*). In this report, we evaluate the significance of these residues to MDD function and demonstrate both similarities and contrasts between the function of this enzyme and other members of the GHMP kinase superfamily of proteins.

EXPERIMENTAL PROCEDURES

Materials. The pSKB2 plasmid containing full-length cDNA for yeast MDD and a histidine tag upstream of the N terminus of the enzyme was a gift from Drs. S. Burley and M. Romanowski (Rockefeller University). Deoxyoligonucleotides used for the mutagenic substitutions were synthesized by Operon Technologies. The *Escherichia coli* strain BL-21 (DE3) used for transformation was obtained from Novagen. Isopropyl-β-D-thiogalactopyranoside was purchased from Research Products International Corp. TNP-

† This work was supported in part by NIH DK53766.

* Corresponding author. Phone: (816) 235-2246. Fax: (816) 235-5595. E-mail: miziorkoh@umkc.edu.

[1] Abbreviations: MDD, mevalonate diphosphate decarboxylase; MK, mevalonate kinase; GHMP, galactokinase, homoserine kinase, mevalonate kinase, phosphomevalonate kinase; MPP, mevalonate diphosphate/pyrophosphate; DPGP, diphosphoglycolylproline; TEAB, triethylammonium bicarbonate.

10.1021/bi0484217 CCC: $30.25
Published on Web 01/25/2005

ATP (2′(3′)-*O*-(2,4,6-trinitrophenyl)adenosine 5′-triphosphate) is a product of Molecular Probes. Kits for DNA purification were products of QIAGEN Inc. Ni−NTA agarose was purchased from QIAGEN Inc. All other biochemical reagents were purchased from Sigma. Mevalonolactone and trimethylsilyl iodide were purchased from Aldrich. [2-^{14}C]mevalonic acid lactone, used for enzymatic synthesis of [2-^{14}C]mevalonate 5-diphosphate (*12*, *13*) was purchased from Moravek Biochemicals. Diphosphoglycolylproline was synthesized from methylproline (Aldrich) by the method of Vlattas et al. (*14*).

Expression and Isolation of Recombinant Wild-Type and Mutant Yeast MDD Proteins. A full circle PCR method, which employed a Stratagene QuikChange site-directed mutagenesis protocol, was used to generate desired mutations. The following primers were used: S34A, 5′-TGCCCACCAATTCGGCCATATCAGTGACTTT-3′ and 5′-AAAGTCACTGATATGGCCGAATTGGTGGGCA-3′; S36A, 5′-ACCAATTCGTCCATAGCAGTGACTTTATCGCA-3′ and 5′-TGCGATAAAGTCACTGCTATGGACGAATTGGT-3′; S120A, 5′-GCAGCTGGTTTAGCTGCCTCCGCTGCTGGCTTTGC-3′ and 5′-GCAAAGCCAGCAGCGGAGGCAGCTAAACCAGCTGC-3′; S121A, 5′-CAGCTGGTTTAGCTTCCGCCGCTGCTGGCTTTGC-3′ and 5′-GCAAAGCCAGCAGCGGCGGAAGCTAAACCAGCTG-3′; S153A, 5′-AATAGCAAGAAAGGGGGCTGGTTCAGCTTGTA-3′ and 5′-TACAAGCTGAACCAGCCCCCTTTCTTGCTATT-3′; S155A, 5′-AAGAAAGGGGTCTGGTGCAGCTTGTAGATCGTT-3′ and 5′-AACGATCTACAAGCTGCACCAGACCCCTTTCTT-3′.

The presence of the desired mutation and the absence of any unanticipated changes in coding sequence were confirmed by automated DNA sequencing. DNA was sequenced at the Protein and Nucleic Acid Shared Facility at the Medical College of Wisconsin. The conditions for high-yield expression/purification of the yeast MDD have been previously reported (*6*) and are briefly summarized. *E. coli* transformants containing the pSKB2 construct were grown in 1 L of LB medium at 25 °C. Protein production was induced by addition of 1 mM isopropyl-β-D-thiogalactopyranoside when the A_{600} reached 1.5; bacteria were harvested after 10 h of induction. The cells were suspended and lysed by passage through a French pressure cell at 16 000 psi. The lysate was centrifuged at 100 000*g* for 1 h, and the supernatant was dialyzed against 10 L of 20 mM Tris/Cl buffer at pH 7.4, containing 0.5 mM DTT. The dialyzed supernatant was loaded onto a 10 mL Ni−NTA agarose column equilibrated with the same buffer. The column was washed until A_{280} was <0.015, and MDD was eluted with a 10−200 mM linear gradient of imidazole in 10 mM Tris/Cl, 100 mM NaCl, 0.5 mM DTT, pH 7.0. The fractions containing MDD were pooled and concentrated using an Amicon YM-10 filter and concentration device (Millipore). The buffer was exchanged to 10 mM Tris/Cl, 0.5 mM DTT, pH 7.0, by repeated concentration of the protein and dilution using this buffer. The concentration of the protein was determined spectrophotometrically using an extinction coefficient ($\epsilon_{280\,nm}$ = 55 340 M^{-1} cm^{-1}) calculated from the deduced protein composition. Glycerol was added to final concentration of 20% and enzyme was frozen and stored at −80 °C for further use. Freezing under these conditions did not affect the activity of the enzyme.

TNP-ATP Binding to Wild-Type and Mutant MDD Proteins. The recombinant wild-type and mutant enzymes were tested for structural integrity using trinitrophenyl-ATP (TNP-ATP), a fluorescent analogue of ATP. The fluorescence enhancement of TNP-ATP upon binding to MDD was measured in 100 mM Tris/Cl, 100 mM NaCl, 10 mM $MgCl_2$, pH 7.0, using a PTI spectrofluorimeter. Excitation wavelength used in these experiments was 408 nm. Emission spectra were scanned from 500 to 600 nm. For data analysis, values measured at the fluorescence emission peak of 540 nm for enzyme-bound TNP-ATP were corrected for free TNP-ATP fluorescence. Thus, the fluorescence enhancement was used in all binding analyses. In the case of all MDD proteins, the emission peak was observed at 540 nm. Titrations of MDD proteins were performed using an enzyme site concentration of 2 μM and TNP-ATP concentrations ranging from 0 to 10 μM. The intensity of the fluorescence enhancement indicated the concentration of bound TNP-ATP; free TNP-ATP was calculated by subtraction of bound ligand from the total added. The titration data were subjected to Scatchard analysis using the Grafit program. Binding stoichiometries (n) were estimated from the calculated x-axis intercepts of the Scatchard plots, and equilibrium binding constants (K_d) were estimated from the slopes of the lines fitted to the data.

Kinetic Characterization of Wild-Type and Mutant Enzymes. Measurement of enzyme activity was typically carried out in the presence of 10 mM $MgCl_2$ at 30 °C, pH 7.0; product ADP formation was measured using a spectrophotometric assay previously described (*15*). The initial velocity was determined on the basis of the rate of decrease in absorbance at 340 nm following addition of mevalonate diphosphate to the reaction mixture. One unit of enzyme activity corresponds to conversion of 1 μmol of substrate to product in 1 min.

When the catalytic efficiency of a mutant enzyme was low, activity was measured using a radioisotope assay (*5*,*16*). The radiolabeled substrate [2-^{14}C]mevalonate diphosphate required for the assay was synthesized enzymatically from [2-^{14}C]mevalonic acid lactone as previously described (*12*, *13*). Recombinant forms of mevalonate kinase (*17*, *18*) and phosphomevalonate kinase (T. Herdendorf and H. Miziorko, unpublished observations) were employed for this synthesis. C18 Sep-Pak cartridges (Waters) were used for separation of the radiolabeled product, isopententyl diphosphate, from substrate. Radioactivity measurements were made using a Beckman LS3801 scintillation counter. For estimates of the maximum velocity (V_{max}) and Michaelis constant (K_m), the reaction velocities at various substrate concentrations were fit to the Michaelis−Menten equation using the Grafit program (Erithacus Software Ltd.).

The potential inhibitor diphosphoglycolylproline (1-({[(phosphonatooxy)phosphinato]oxy}acetyl)pyrrolidine-2-carboxylate) was synthesized using the strategy briefly outlined by Vlattas et al. (*14*). Two millimoles of L-proline methyl ester was dissolved in 1 M $NaHCO_3$. Then 0.5 mL of $ClCH_2COBr$ was added dropwise with stirring on ice. The reaction was allowed to continue for 2 h at room temperature. The reaction mixture was then acidified by dropwise addition of 2 M HCl to pH ∼3. The product, 1-(2-bromoacetyl)-pyrrolidine-2-carboxylic acid methyl ester, was extracted with dichloromethane and dried for 2 h by the addition of

anhydrous $MgSO_4$, filtered thorough Whatman #1 filter paper, and concentrated using a rotary evaporator. This intermediate was purified by silica gel chromatography (2 × 20 cm column); elution was performed with 50:1 (CH_2Cl_2:MeOH). The purified intermediate was concentrated by rotary evaporation and characterized by the ^1H NMR spectroscopy. A solution of this material in dry acetonitrile was added to tetrabutylammonium pyrophosphate in the same solvent. The reaction was conducted under a N_2 atmosphere for 3.5 h at room temperature. The acetonitrile was removed using rotary evaporation, and the reaction product, 1-({[(phosphonatooxy)phosphinato]oxy}acetyl)pyrrolidine-2-carboxylic acid methyl ester, was dissolved in 10 mL of water and loaded to the Dowex 50W column (NH_4^+ form) and eluted with water. This material was applied to a DEAE Sephadex A25 (5 × 15 cm) column, equilibrated with triethylammonium bicarbonate (TEAB) buffer (pH 7.5), and eluted with a gradient of TEAB (20−500 mM; total volume of 1600 mL). Fractions were detected with $FeCl_3$/sulfosalicylic acid spray as previously described (*19*). Pooled product fractions were concentrated to dryness three times from acetonitrile and characterized by ^1H and ^{31}P NMR. The material was dissolved in 5 mL of water and applied to a Dowex 50W (Li^+ form) column, eluted with water, and concentrated using rotary evaporation. The methyl ester was hydrolyzed with 0.5 M LiOH overnight at 4 °C. The pH was then adjusted with dropwise addition of HCl to neutrality. The deesterified product, diphosphoglycolylproline (1-({[(phosphonatooxy)phosphinato]oxy}acetyl)pyrrolidine-2-carboxylate) was lyophilized and stored at −80 °C. Observed peaks and chemical shifts in ^1H, ^{13}C, and ^{31}P NMR spectra were identical to those previously reported (*14*). The concentration of the diphosphoglycolylproline was determined by organic phosphate analysis (*20*).

Tests of the efficacy of inhibition were conducted using the standard spectrophotometric assay in the presence of different concentrations of diphosphoglycolylproline. The slopes from double-reciprocal plots were fitted as a function of diphosphoglycolylproline concentration. $K_{i(slope)}$ values were calculated using the Grafit program (Erithacus Software Ltd.).

EPR Spectroscopy. To test whether the His-tag influenced the metal binding properties of the protein, the gene construct was reengineered into the pET11a vector (Stratagene) using *Nde*I and *Bam*HI restriction enzymes (New England Biolabs). The untagged yeast mevalonate diphosphate decarboxylase enzyme was expressed in BL21 (DE3) *E. coli* and purified as earlier reported (*4*) to 80% purity as judged by SDS−PAGE and the standard activity assay (*15*). The protein was twice dialyzed against 8 L of 20 mM Tris/Cl, 100 mM NaCl, pH 7.2 buffer, containing 1 mM EDTA to remove adventitious metals and then dialyzed three times against the same buffer without EDTA. Untagged MDD, as well as homogeneous His-tagged MDD was prepared in 20 mM Tris/Cl, 100 mM NaCl, pH 7.2, 10% glycerol. Samples (300 μL) were titrated with small aliquots of Mn^{2+} or Mn^{2+}−substrate complex and frozen in liquid N_2. The formation of any complex of Mn^{2+} with ATP, mevalonate 5-diphosphate, or MDD was tested by means of Mn^{2+} EPR spectroscopy using a Varian E109 Century Series spectrometer equipped with a TE102 cavity. X-band (8.9−9.4 GHz) EPR spectra were recorded for each sample in a 4-mm OD quartz EPR tube inserted into a finger Dewar filled with liquid N_2 (at 77 K). The enzyme remained fully active after freezing−thawing cycles as confirmed by standard enzymatic assay. Additional experiments performed on His-tagged MDD in solution state (22 °C) using a quartz flat cell confirmed the results obtained with frozen samples.

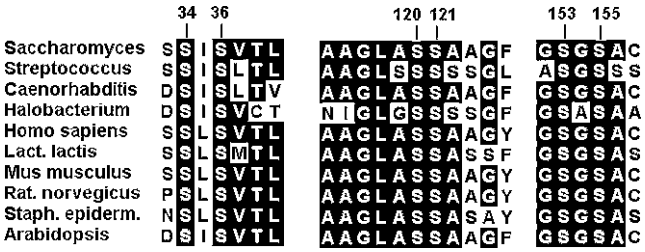

FIGURE 1: Invariant serine residues in the interdomain cleft of mevalonate diphosphate decarboxylases. Amino acid sequences of 10 eukaryotic and prokaryotic proteins were aligned using the Bioedit program. Numbers appearing above the sequence alignment correspond to the conserved serine residues of *Saccharomyces cerevisiae*. Sequences corresponding to the following organisms and accession numbers are included: *Saccharomyces cerevisiae*, P32377; *Streptococcus pyogenes* M1 GAS, AAK33797; *Caenorhabditis elegans*, NP_496967; *Halobacterium* sp. NRC-1, D84217; *Homo sapiens*, P53602; *Lactococcus lactis*, E86675; *Mus musculus*, CAC35731; *Rattus norvegicus*, AAB00192; *Staphylococcus epidermis*, BAB56753; *Arabidopsis thaliana*, T52625.

RESULTS

Mutagenic Substitution of Alcohol Side Chains. There is strong precedent for participation of alcohol functionalities in phosphotransferase substrate binding and/or catalysis. A potential active site role for such residues involves H-bonding to oxygens of the ATP phosphoryl chain (*9*, *21*−*23*). Elimination of side chains that function in phosphoryl chain orientation by hydrogen-bonding interactions can correlate with large diminutions in catalytic rate (*10*, *11*).

The structure of unliganded yeast MDD (*7*) exhibits an interdomain cleft associated with Mg-ATP binding in other enzymes in the GHMP kinase family, and it seems reasonable that serine/threonine residues that have roles in either of the two functions described above should map in the vicinity of this cleft. Alignment of deduced sequences for eukaryotic and prokaryotic MDD proteins (Figure 1) indicates several strictly invariant residues (Ser-34, Ser-36, Ser-120, Ser-121, Ser-153, Ser-155) that fulfill such a criterion. On the basis of the probability that one or more of these residues has an active site function, a direct test of such function seemed worthwhile. To support this objective, PCR-based mutagenesis (Stratagene Quick Change protocol) was employed to produce histidine-tagged proteins in which each of these residues was replaced with alanine. Mutant proteins were expressed in *E. coli* and extracted and isolated using a nickel affinity resin as previously reported (*6*). The expression of S34A as well as S208 A (Ser-208 is highly conserved in MDD proteins) as judged from total protein lysates was comparable to wild-type MDD and the other mutants. However, little of these proteins remained soluble after ultracentrifugation and they were not characterized in detail. All other mutants were recovered in good yield in the soluble fraction, isolated by Ni−NTA agarose chromatography in highly homogeneous form, and, upon SDS−PAGE, exhibited the same subunit molecular mass (48 kDa) that has been observed for wild-type yeast MDD.

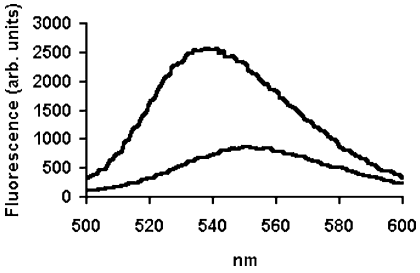

FIGURE 2: Fluorescence enhancement of TNP-ATP upon binding to yeast mevalonate diphosphate decarboxylase. The lower spectrum represents 10 μM TNP-ATP recorded in 10 mM Tris/Cl, 100 mM NaCl, 10 mM $MgCl_2$, pH 7.0. The upper spectrum represents the fluorescence emission ($\lambda_{max} \sim 540$ nm) of a sample containing 10 μM TNP-ATP and 3.8 μM S121A after correction (subtraction) for the amplitude of the signal (lower spectrum) measured for TNP-ATP under the same buffer conditions; i.e., the emission from the TNP-ATP itself was subtracted from the original uncorrected enzyme−TNP-ATP spectrum. Excitation wavelength used in these experiments is 408 nm.

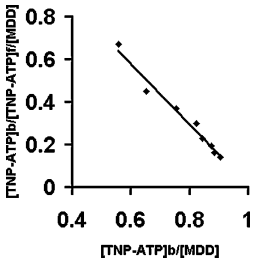

FIGURE 3: Scatchard plot of the data for TNP-ATP binding to S121A MDD protein. $[TNP\text{-}ATP]_b$ and $[TNP\text{-}ATP]_f$ represent the concentration of bound and free TNP-ATP, respectively. [MDD] indicates the subunit concentration of S121A MDD. Titration of S121A protein was performed using an enzyme site concentration of 2 μM and TNP-ATP concentrations ranging from 0 to 10 μM. The intensity of the fluorescence enhancement indicated the concentration of bound TNP-ATP; free TNP-ATP was calculated by subtraction of bound ligand from the total TNP-ATP added. The titration data were subjected to Scatchard analysis using the Grafit program (Erithacus Sotware Ltd).

Biophysical Characterization of Wild-Type and Mutant Mevalonate Diphosphate Decarboxylase Proteins. A fluorescent ATP analogue, trinitrophenyl-ATP (TNP-ATP), has been used to evaluate the structural integrity of various wild-type and mutant phosphotransferases and also proves useful in testing the ATP binding site in MDD (*24*). Upon addition of the enzyme to the TNP-ATP, the maximum emission increases in intensity and shifts in wavelength from 555 to 540 nm, indicating the binding of the analogue to the wild-type and mutant enzymes (e.g., S121A; Figure 2). The "blue shift" of the emission spectra to 540 nm for each MDD protein indicates a relatively hydrophobic binding site for TNP-ATP. The stoichiometry for TNP-ATP binding to wild-type and mutant MDD proteins is obtained from the *x*-axis intersection points of Scatchard plots of the binding data; equilibrium binding constants are calculated from the slopes (Figure 3 depicts data for S121A). Mutants with alanine substitutions for serine residues 34, 36, 120,121, 153, and 155 were investigated. S34A did not bind the TNP-ATP with affinity of the type reported for wild-type enzyme or other serine mutants. This observation, together with the limited recovery of soluble protein from bacterial lysates, suggests that S34A may not fold like wild-type protein. Similar observations were made for the alanine mutant in which a highly conserved Ser-208 is replaced. Values for binding stoichiometry and affinity have been measured for wild-type and the other mutant MDD proteins (S36A, S120A, S121A, S153A, and S155A) (Table 1). Binding stoichiometries measured for mutant enzymes are within 30% of the value documented for wild-type enzyme. These observations indicate that the mutants retain substantial structural integrity. Affinity for substrate Mg-ATP was measured in competitive displacement experiments (*25*) where Mg-ATP is used to displace the fluorescent TNP-ATP. The binding constants for Mg-ATP to wild-type and several mutant MDDs are summarized in Table 1. The dissociation constants for S36A, S120A, S121A, and S155A with Mg-ATP are only slightly (<3.6-fold) higher than for the wild-type enzyme. The biggest effect (≈18-fold) is observed for the S153A mutant. For this mutant, the affinity for TNP-ATP is also diminished (7-fold). On the basis of these data, serine-153 appears to support binding of Mg-ATP at the MDD active site.

Table 1: Summary of Equilibrium Binding Parameters for Wild-Type and Mutant MDD Enzymes to Substrate Analogue TNP-ATP and to ATP[a]

enzyme	$K_{d(TNP-ATP)}$, μM	n[b]	$K_{d(Mg-ATP)}$, μM
wild-type[c]	0.49 ± 0.04	1.07 ± 0.11	169 ± 17
S36A	0.68 ± 0.05	0.8 ± 0.1	502 ± 35
S120A	0.61 ± 0.04	1.06 ± 0.09	531 ± 37
S121A	0.7 ± 0.1	1.00 ± 0.08	615 ± 14
S153A	3.4 ± 0.2	0.97 ± 0.07	2980 ± 213
S155A	0.62 ± 0.04	0.86 ± 0.08	371 ± 27

[a] K_d for TNP-ATP and Mg-ATP with MDD was measured in 100 mM Tris/HCl, 100 mM NaCl, pH 7.4, in the presence of 10 mM $MgCl_2$ at 30 °C. $K_{d(TNP-ATP)}$ was calculated by titration of the enzyme with TNP-ATP. $K_{d(Mg-ATP)}$ was calculated in competitive displacement experiments by titration of the TNP-ATP−enzyme complex with Mg-ATP. [b] The *n* values for the TNP-ATP binding to wild-type and mutant MDD proteins were obtained from the calculated *x*-axis intersection points of the Scatchard plots. [c] Data for wild-type were previously reported (*6*).

In other biophysical characterization experiments, electron spin resonance measurements have been performed to evaluate binding of Mn^{2+} (which supports 80% of the activity of recombinant yeast MDD measured using Mg^{2+} in the standard assay) to substrate and protein. Titration of mevalonate 5-diphosphate (in 20 mM Tris-Cl, pH 7.2 with 100 mM NaCl, and 10% glycerol; measurements performed at 77 K) with Mn^{2+} produces a six-line spectrum typical of Mn^{2+}, while in the absence of mevalonate 5-diphosphate no substantial signal was observed for comparable levels of cation in these buffered, glycerol-containing, frozen samples. Signal amplitude data, which reflect the concentration of metabolite-bound cation, are compatible with a hyperbolic saturation curve and suggest stoichiometric binding of cation to mevalonate 5-diphosphate with a $K_d = 13.6$ μM. In contrast, similar titrations of His-tagged or untagged enzyme with Mn^{2+} did not suggest specific, high-affinity binding to MDD protein in the absence of substrate. This observation is also supported by experiments, performed at 22 °C, in which His-tagged MDD was titrated with Mn^{2+} and the signal amplitude compared with measurements made using protein-free buffered control samples. No significant Mn^{2+} binding to enzyme (detectable as reduced ESR peak amplitude) could be detected.

Kinetic Characterization of Mutant Mevalonate Diphosphate Decarboxylase Proteins. Since S34A (also S208A) did

Table 2: Kinetic Constants of Wild-Type and Mutant Mevalonate Diphosphate Decarboxylases[a]

enzyme	V_{max}, units/mg	$K_{m(D,L-MPP)}$, μM	$K_{m(Mg-ATP)}$, μM	k_{cat}, s^{-1}	$k_{cat}/K_{m(D,L-MPP)}$, $s^{-1}\,\mu M^{-1}$	$k_{cat}/K_{m(Mg-ATP)}$, $s^{-1}\,\mu M^{-1}$
wild-type	6.4 ± 0.2	123 ± 22	61 ± 6	4.9	4×10^{-2}	8×10^{-2}
S36A	4.36 ± 0.13	307 ± 22	65 ± 2	3.35	1.1×10^{-2}	5.15×10^{-2}
S120A	0.80 ± 0.01	267 ± 12	525 ± 61	0.61	2.3×10^{-3}	1.17×10^{-3}
S121A	$(1.5 \pm 0.1) \times 10^{-4}$	95 ± 12		1.15×10^{-4}	1.2×10^{-6}	
S153A	2.19 ± 0.06	944 ± 53	2172 ± 265	1.68	1.8×10^{-3}	7.7×10^{-4}
S155A	0.85 ± 0.08	1921 ± 287	1592 ± 188	0.65	3.4×10^{-4}	4.1×10^{-4}

[a] Kinetic properties of wild-type and some of the mutant MDDs were measured in 100 mM Tris/HCl, 100 mM KCl, pH 7.0 in the presence of 10 mM $MgCl_2$ at 30 °C. Data for wild-type enzyme have been previously reported (6).

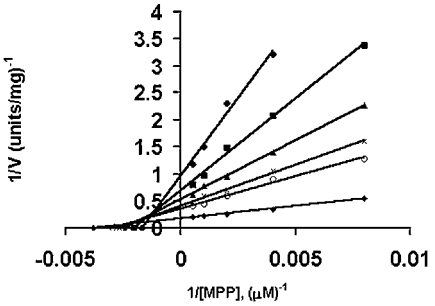

FIGURE 4: Inhibition of wild-type MDD by diphosphoglycolylproline. The rate and substrate concentration data were analyzed as double reciprocal plots. The concentrations of diphosphoglycolylproline used were 0 μM (◆), 43 μM (○), 87.5 μM (×), 171.5 μM (▲), 343 μM (■), 686 μM (●). The concentration of the MPP varied from 62.5 to 2000 μM. The rates of the reaction were measured using the standard spectrophotometric assay.

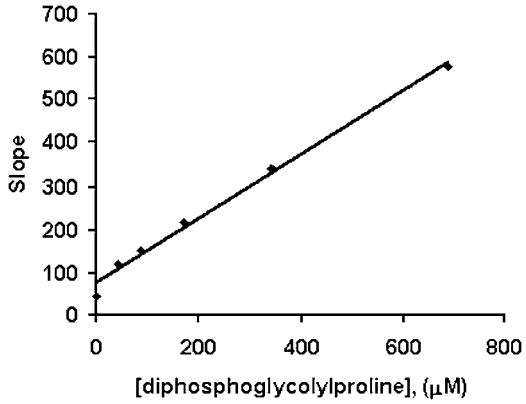

FIGURE 5: Calculation of the $K_{i(slope)}$ for wild-type MDD. $K_{i(slope)}$ was measured by plotting the slopes of double reciprocal plots (Figure 4) versus the concentration of diphosphoglycolylproline (0, 43, 87.5, 171.5, 343, 686 μM). The constants were calculated using the Grafit program (Erithacus Software).

not persist as a soluble, stable protein, kinetic characterization has been limited to S36A, S120A, S121A, S153A, and S155A mutant enzymes. Comparison of k_{cat} and substrate K_m kinetic parameters with values measured for wild-type recombinant His-tagged yeast MDD is provided in Table 2. In addition, diphosphoglycolylproline has been reported to inhibit animal MDD (*14*); this observation has been tested (Figure 4) with the recombinant yeast enzyme. For the yeast protein, linear noncompetitive (mixed) inhibition is observed. $K_{i(slope)}$ values (Figure 5) are reported for wild-type and several mutant enzymes in Table 3. The low activity of S121A precluded inhibition studies with this mutant. With the exception of S121A, substitutions of alanine for serine change catalytic rates by less than 1 order of magnitude. Notable changes in substrate K_m include a 35-fold inflation

Table 3: Inhibition of Wild-Type and Serine MDD Mutants by Diphosphoglycolylproline

enzyme	$K_{i(slope)}$,[a] μM
wild-type	105 ± 16
S36A	66 ± 6
S120A	18 ± 14
S153A	1576 ± 93
S155A	1429 ± 63

[a] $K_{i(slope)}$ values were measured by plotting the slopes of the double reciprocal plots (Figure 4) versus the concentration of diphosphoglycolylproline (0, 43, 87.5, 171.5, 343, 686 μM). The constants were calculated using the Grafit program (Erithacus Software Ltd.).

in $K_{m(Mg-ATP)}$ for S153A; this effect is comparable in magnitude to the 18-fold inflation in $K_{d(Mg-ATP)}$ measured for this mutant (Table 1). Together, these results suggest impaired interaction with Mg-ATP when the side chain of Ser-153 is absent. In contrast, the 26-fold inflation in $K_{m(Mg-ATP)}$ observed for S155A (Table 2) is not matched by the 2-fold change in $K_{d(Mg-ATP)}$. This raises some uncertainty concerning whether Ser-155 makes an important contribution to binding of the Mg-ATP substrate. For S155A, the 16-fold inflation in $K_{m(MPP)}$ is approximately matched by the 14-fold inflation in $K_{i(slope)}$ for the inhibitor diphosphoglycolylproline (Table 3) which should reflect this mutant's impaired ability to form a binary EI complex with the phosphorylated inhibitor. This correlation raises the possibility that the side chain of Ser-155 supports interaction with the phosphoryl acceptor substrate, mevalonate diphosphate. The effects of the S153A mutation on mevalonate diphosphate binding are somewhat more complicated. The inflation in $K_{m(MPP)}$ is less than 8-fold, while the inflation in $K_{i(slope)}$ for diphosphoglycolylproline (15-fold; Table 3) is somewhat larger. These changes are not as self-consistent as effects measured for Mg-ATP, complicating evaluation of the possibility that Ser-153 also contributes to enzyme interaction with the phosphoryl acceptor. $K_{i(intercept)}$ values have also been estimated for these MDD proteins from linear replots of intercept versus inhibitor concentration. The values (wild-type, $K_{i(intercept)} = 383 \pm 33$ μM; S153A, $K_{i(intercept)} = 687 \pm 225$ μM; S155A, $K_{i(intercept)} = 160 \pm 62$ μM), which reflect formation of a nonproductive E−mevalonate 5-diphosphatate−inhibitor complex, do not show any correlation with the $K_{m(MPP)}$ values for these enzymes.

In contrast with the modest effects on k_{cat} observed for most of the mutants, the 42 000-fold diminution measured for S121A seems noteworthy. This mutation produces little effect on $K_{m(MPP)}$. $K_{m(Mg-ATP)}$ cannot be accurately measured at subsaturating Mg-ATP concentrations, due to slow but substantial ATP hydrolysis during the long incubation times required for measuring the catalytically deficient mutant.

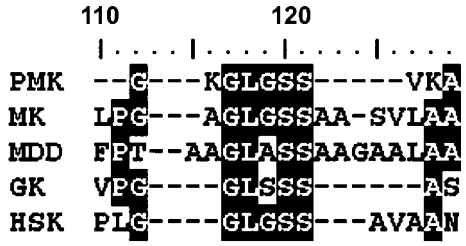

FIGURE 6: Similarity between glycine/serine-rich loop (motif 2) sequences in the GHMP kinase superfamily of proteins. The consensus sequences for the members of GHMP kinase superfamily were generated after the alignment of the eukaryotic and prokaryotic proteins using the Bioedit program. The following sequences were adopted to calculate consensus. MDD (mevalonate diphosphate decarboxylase): *L. lactis*, *A. thaliana*, *Caenorhabditis elegans*, *Halobacterium*, *H. sapiens*, *M. musculus*, *R. norvegicus*, *S. cerevisiae*, *Staphylococcus epidermidis*, *Streptococcus*, *Thermoplasma volcanium*. MK (mevalonate kinase): *A. thaliana*, *H. sapiens*, *L. lactis*, *M. musculus*, *R. norvegicus*, *S. cerevisiae*. PMK (phosphomevalonate kinase): *S. pyogenes*, *S. aureus*, *S. cerevisiae*, *Lactobacillus helveticus*, *H. sapiens*, *Enterococcus faecalis*. GK (galactokinase): *A. thaliana*, *E. faecalis*, *E. coli*, *H. sapiens*, *M. musculus*, *S. cerevisiae*, *Streptococcus pneumoniae*. HSK (homoserine kinase): *A. thaliana*, *Bordetella bronchiseptica*, *E. coli*, *S. cerevisiae*, *S. epidermidis*.

However, interaction of S121A with Mg-ATP substrate does not seem impaired on the basis of the measured K_d value for Mg-ATP (Table 1), which is only 3.6-fold higher than the estimate for wild-type enzyme. Together, these data suggest a critical role for the alcohol side chain of Ser-121 in catalysis of the mevalonate diphosphate decarboxylase reaction.

DISCUSSION

While Ser-34 and Ser-208 are either invariant or highly conserved in deduced sequences proposed to correspond to mevalonate diphosphate decarboxylases, replacement of these residues with alanine leads to unstable proteins. Their structural importance is clear, but it is not possible to evaluate whether they have additional important roles in substrate binding or catalysis. In contrast, Ser-120 and Ser-121, residues which map in the highly conserved "motif 2" of the GHMP kinase family (*26*), are amenable to more thorough analysis. The data indicate that the second serine in this motif, Ser-121, is clearly much more critical to function, since substitution that eliminates the side chain hydroxyl diminishes the catalytic rate by >42 000-fold. By analogy with results for homologous serine residues in mevalonate kinase (*11*, *21*), which indicate a major role for Ser-146 but a minimal role for adjacent Ser-145, the proposal that Ser-121 in mevalonate diphosphate decarboxylase functions in orienting the phosphoryl chain to optimize the angle of attack on the γ-phosphoryl seems plausible.

Also noteworthy is the contrasting modest 8-fold k_{cat} effect measured for S120A. This discrimination between the two sequential serines is reminiscent of the effects measured for mevalonate kinase, where the functional contribution of Ser-146 is much larger than that of Ser-145. Since two or more tandem alcohol-containing side chains are frequently documented in the "motif 2" region of GHMP kinases (Figure 6), it will be interesting to learn whether other enzymes in the family that contain tandem alcohols in this sequence motif also exhibit such specificity in the magnitude of functional contributions.

In considering roles for other functionally important invariant serines in mevalonate diphosphate decarboxylase, no insight from homology patterns is available. Ser-153 and Ser-155 are situated in a turn between two α-helices (*7*) and other GHMP kinases do not appear to contain comparable side chains at these positions. Thus, Ser-153 and Ser-155 may make a substantial contribution to defining the specificity for the MDD reaction. In the context of speculating about particular roles for these residues, Ser-153 clearly interacts with Mg-ATP, based on mutagenesis effects on K_d and K_m for this substrate. In the case of homoserine kinase, the alcohol side chain of Thr-183 (which, like MDD Ser-153 is downstream of the serine residues in homoserine kinase's "motif 2"; Figure 6) has been shown (*27*) to interact with the β-phosphoryl of ATP.

For Ser-155, how may the interaction with mevalonate 5-diphosphate and the analogue diphosphoglycolyl proline best be rationalized? Both acceptor substrate and inhibitor molecules contain a diphosphate moiety. Hydrogen-bonding interactions between the Ser-155 alcohol proton and the substrate/inhibitor nonbridging phosphoryl oxygens could account for the inflation in $K_{m(MPP)}$ and $K_{i(slope)}$ observed with the S155A mutant. Reexamination of the corresponding residues in animal MDD, where a simpler inhibition pattern may be observed (N. Voynova and H. Miziorko, unpublished observations), could clarify the role of Ser-155. However, any extrapolation from kinetic parameters measured under steady-state turnover conditions to binding affinity that might be reflected by binding constants measured in equilibrium binding experiments on binary enzyme−substrate or enzyme−inhibitor samples is not always straightforward. Thus, the function of Ser-155, which seems to influence enzyme specificity, remains less obvious than roles discussed above for Ser-153 and Ser-121.

ACKNOWLEDGMENT

Dmitriy Krepkiy is the recipient of a postdoctoral fellowship from the American Heart Association. The help of Dr. Chang-Zeng Wang with the synthesis of diphosphoglycolylproline is appreciated.

REFERENCES

1. Alvear, M., Jabalquinto, A. M., Eyzaguirre, J., Cardemil, E. (1982) Purification and characterization of avian liver mevalonate-5-pyrophosphate decarboxylase, *Biochemistry 21*, 4646−4650.
2. Jabalquinto, A. M. and Cardemil, E. (1987) Kinetic effects of ATP, divalent metal ions and pH on chicken liver mevalonate 5-diphosphate decarboxylase, *Biochim. Biophys. Acta 916*, 172−178.
3. Nave, J. F., d'Orchymont, H., Ducep, J. B., Piriou, F., Jung, M. J. (1985) Mechanism of the inhibition of cholesterol biosynthesis by 6-fluoromevalonate, *Biochem. J. 227*, 247−254.
4. Reardon, J. E., and Abeles, R. E. (1987) Inhibition of cholesterol biosynthesis by fluorinated mevalonate analogues, *Biochemistry 26*, 4717−4722.
5. Sawamura, M., Nara, Y., Yamori, Y. (1992) Liver mevalonate 5-pyrophosphate decarboxylase is responsible for reduced serum cholesterol in stroke-prone spontaneously hypertensive rat, *J. Biol. Chem. 267*, 6051−6055.
6. Krepkiy, D., and Miziorko, H. M. (2004) Identification of active site residues in mevalonate diphosphate decarboxylase: Implications for a family of phosphotransferases, *Protein Science 13*, 1875−1881.
7. Bonanno, J. B., Edo, C., Eswar, N., Pieper, U., Romanowski, M. J., Ilyin, Y., Gerchman, S. E., Kycia, H., Studier, F. W., Sali, A.,

and Burley, S. K. (2001) Structural genomics of enzymes involved in sterol/isoprenoid biosynthesis, *Proc. Natl. Acad. Sci. U.S.A. 98*, 12896−12901.
8. Smith, C. A., and Rayment, I. (1996) Active site comparisons highlight structural similarities between myosin and other P-loop proteins, *Biophys. J. 70*, 1590−1602.
9. Hasemann, C. A., Istvan, E. S., Uyeda, K., and Deisenhofer, J. (1996) The crystal structure of the bifunctional enzyme 6-phosphofructo-2-kinase/fructose-2,6-bisphosphatase reveals distinct domain homologies, *Structure 4*, 1017−1029.
10. Uyeda, K., Wang, X. L., Mizuguchi, H., Li, Y., Nguyen, C., Hasemann, C. A. (1997) The active sites of fructose 6-phosphate, 2-kinase: Fructose-2, 6-bisphosphatase from rat testis. Roles of Asp-128, Thr-52, Thr-130, Asn-73, and Tyr-197, *J. Biol. Chem. 272*, 7867−7872.
11. Cho, Y. K., Rios, S. E., Kim, J. J., Miziorko, H. M. (2001) Investigation of invariant serine/threonine residues in mevalonate kinase. Tests of the functional significance of a proposed substrate binding motif and a site implicated in human inherited disease, *J. Biol. Chem. 276*, 12573−12578.
12. Chiew, Y. E., O'Sullivan, W. J., Lee, C. S. (1987) Studies on pig liver mevalonate-5-diphosphate decarboxylase, *Biochim. Biophys. Acta 916*, 271−278.
13. Pilloff, D., Dabovic, K., Romanowski, M. J., Bonanno, J. B., Doherty, M., Burley, S. K., Leyh, T. S. (2003) The kinetic mechanism of phosphomevalonate kinase, *J. Biol. Chem. 278*, 4510−4515.
14. Vlattas, I., Dellureficio, J., Ku, E., Bohacek, R., Zhang, X. (1996) Inhibition of mevalonate 5-pyrophosphate decarboxylase by a proline-containing transition state analogue, *Bioorg. Med. Chem. Lett. 6*, 2091−2096.
15. Cardemil, E., and Jabalquinto, A. M. (1985) Mevalonate 5-pyrophosphate decarboxylase from chicken liver, *Methods Enzymol. 10*, 86−92.
16. Hulcher, F. H. (1991) Modification of the radiochemical assay of rat liver mevalonate-5-diphosphate decarboxylase and induction and stabilization of the activity, *Biochem. Biophys. Res. Commun. 181*, 1449−1455.
17. Potter, D., Miziorko, H. M. (1997) Identification of catalytic residues in human mevalonate kinase, *J. Biol. Chem. 272*, 25449−25454.
18. Potter, D., Wojnar, J. M., Narasimhan, C., Miziorko, H. M. (1997) Identification and functional characterization of an active-site lysine in mevalonate kinase, *J. Biol. Chem. 272*, 5741−5746.
19. Wang, C. Z., and Miziorko, H. M. (2003) Methodology for synthesis and isolation of 5-phosphomevalonic acid, *Anal. Biochem. 321*, 272−275.
20. Hurst, R. O. (1964) The determination of nucleotide phosphorus with a stannous chloride-hydrazine sulphate reagent, *Can. J. Biochem. Physiol. 42*, 287−292.
21. Fu, Z., Wang, M., Potter, D., Miziorko, H. M. and Kim, J. J. (2002) The structure of a binary complex between a mammalian mevalonate kinase and ATP: Insights into the reaction mechanism and human inherited disease, *J. Biol. Chem. 277*, 18134−18142.
22. Hartley, A., Glynn, S. E., Barynin, V., Baker, P. J., Sedelnikova, S. E., Verhees, C., de Geus, D., van der Oost, J., Timson, D. J., Reece, R. J., Rice, D. W. (2004) Substrate specificity and mechanism from the structure of Pyrococcus furiosus galactokinase, *J. Mol. Biol. 337*, 387−398.
23. Miallau, L., Alphey, M. S., Kemp, L. E., Leonard, G. A., McSweeney, S. M., Hecht, S., Bacher, A., Eisenreich, W., Rohdich, F., Hunter, W. N. (2003) Biosynthesis of isoprenoids: Crystal structure of 4-diphosphocytidyl-2C-methyl-D-erythritol kinase, *Proc. Natl. Acad. Sci. U.S.A. 100*, 9173−9178.
24. Bagshaw, C. R., and Harris, D. A. (1988) Measurement of ligand binding to proteins, In "Spectrophotometry and Spectrofluorimetry" (Harris, D. A. and Bashford, C. L., Eds.) pp 91−113, IRL Press, Washington, DC.
25. Mildvan, A. S., and Cohn, M. (1965) Kinetic and magnetic resonance studies of the pyruvate kinase reaction. I. Divalent metal complexes of pyruvate kinase, *J. Biol. Chem. 240*, 238−246.
26. Bork, P., Sander, C., Valencia, A. (1993) Convergent evolution of similar enzymatic function on different protein folds: The hexokinase, ribokinase, and galactokinase families of sugar kinases, *Protein Sci.* 2, 31−40.
27. Krishna, S. S., Zhou, T., Daugherty, M., Osterman, A., and Zhang, H. (2001)Structural basis for the catalysis and substrate specificity of homoserine kinase, *Biochemistry 40*, 10810−10818.
28. Geeganage, S., Ling, V. W. K., and Frey, P. A. (2000) Roles of two conserved amino acid residues in the active site of galactose-1-phosphate uridylyltransferase: An essential serine and a non-essential cysteine, *Biochemistry 39*, 5397−5404.
29. Dhe-Paganon, S., Magrath, J. and Abeles, R. J. (1994) Mechanism of mevalonate pyrophosphate decarboxylase: Evidence for a carbocationic transition state, *Biochemistry 33*, 13355−13362.

BI0484217